J. B. Gunn

Instabilities of Current in III-V Semiconductors

Abstract: A description is given of a newly discovered phenomenon which is observed when an electric field of a few thousand V cm^{-1} is applied to a homogeneous sample of n-type GaAs or InP. Above a well-defined threshold field, a time-dependent decrease in current is observed, which is largely independent of external circuit conditions. In long specimens this decrease is aperiodic, resembling random noise with a bandwidth of ~10^9 c/sec. In short specimens, coherent oscillations are observed whose period is equal to the transit time of electrons between the ohmic electrodes of the structure. Frequencies over the range 0.5—6.5 Gc/sec have been generated in this way, using experimental techniques which are described. Measurements of the efficiency of dc-to-rf conversion (from 1 to 2%), and of peak power outputs (up to 0.5 W), suggest that the effect may have useful applications. Some diagnostic experiments are described and the results are discussed in terms of various possible mechanisms. Although the quantitative agreement with theory is poor it is concluded that the current instability may possibly be due to the amplification of lattice optical modes.

Introduction

Effects on the bulk electrical properties of semiconductors produced by the application of strong electric fields have been known for some time. Many of these effects reflect changes in the mean energy of the charge carriers, whilst others are associated with the achievement by the carriers of a critical value of drift velocity, or with field-induced changes in the energy band structure. Among the first class may be included changes in drift mobility[1] and electrical noise[2] of the charge carriers, changes in their number due to impact ionization of the lattice[3] or of impurities,[4] and impact recombination at impurity sites.[5] In the second class are current-saturation[6] and "kink"[7] phenomena which are due to the amplification of acoustical waves. The last class is exemplified by Zener tunnelling.[8]

The present paper describes a phenomenon[9] which appears to be new and unrelated to those mentioned above. When a uniform electric field applied to a bulk specimen of *n*-type GaAs is raised above a certain critical value a time-dependent *decrease* in the current is observed. In long specimens this decrease resembles random noise, but in short specimens it is found to be periodic and of an extremely high frequency which is determined by the specimen length. Sufficient microwave power can be transferred to an external load to suggest that the effect may take on technological importance. Similar effects are found in *n*-type InP, but not in *p*-type GaAs.

Section 2 of this paper describes the details of specimen preparation and measurement. Section 3.1 describes the primary experimental findings whilst Section 3.2 gives the results of some diagnostic experiments made in an attempt to uncover the mechanism responsible. Experiments made with applications in mind are discussed in Section 4. The implications of the experiments are discussed in Section 5, even though it is not yet possible to draw any very firm conclusions.

2 Experimental techniques

• *2.1 Specimen preparation*

Two basic geometries of specimen were used, as shown in Figs. 1 and 2. "Long" specimens were cut, from x-ray oriented monocrystalline ingots of semiconductor, in the form of bars approximately 0.5 mm square and 1—10 mm long. A wire saw employing an endless loop of nichrome wire charged with silicon carbide abrasive was used. "Short" specimens were made by first sawing a slice of material of thickness 0.5 mm or less from a polycrystalline or oriented monocrystalline ingot. Both sides were then lapped until a flat wafer of the desired thickness was obtained. Discs 0.8 mm in diameter were then cut by ultrasonic impact grinding using a tool of appropriate shape; even in the case of polycrystalline material, most

Reprinted from
IBM Journal of Research and Development, Vol. 8, No. 2, April 1964

Table 1 **Bulk electrical characteristics of crystals studied.**

Crystal Number	*Material*	*Type*	*Resistivity (ohm–cm)*	*Hall Mobility ($cm^2\ V^{-1}\ sec^{-1}$)*
RC 28303	GaAs	*n*	0.1–1.0	4000–5000
G 133	GaAs	*n*	2–3	5100
52–26	GaAs	*n*	0.3	7610
52–59	GaAs	*p*	0.1	210
InP–2	InP	*n*	0.04	3700
InP–4	InP	*n*	0.3	2000–4000

of the discs cut were free of grain boundaries. In some cases, the discs were lapped again after cutting to reduce their thickness further. After cutting, both types of specimen were degreased and etched in an appropriate etchant: sulphuric-peroxide etch[10a] for GaAs, and methanol-bromine[10b] for InP. They were then rinsed in 5% NaCN to complex any copper present, were then washed in distilled water, and dried in a vacuum dessicator. The bulk electrical characteristics of the crystals used are shown in Table 1.

• *2.2 Electrical contacts*

For the measurements to be reported, electrical contacts were required which, in the presence of a strong electric field, would be linear, noninjecting, geometrically regular, and of low resistance. The last requirement could be met by pressure contacts of In on GaAs. These were used for a few experiments but were unsatisfactory because of their high resistance at low fields and because of ıe . nature of GaAs. Highly doped (n^+ on n, or p^+ on p contacts were more suitable. They were made by he the semiconductor specimen in contact with two 0.8 spheres of an appropriate metal (Sn for n-G .As, Ir f p-GaAs, and pure or doped In or Sn for n-InP). The metal and semiconductor were held in the correct positions by a jig of high-purity graphite which, for the long specimens, took the form of a block with a groove in its upper surface to hold the bar; at each end of the groov formed recesses to hold the molten metal ıe the recesses were slightly tapered so that the a metal was forced by gravity against the semico Each disc specimen (Fig. 2a) was placed, with sphere above and below, in a vertical hole i graphite block. A weighted plunger closing the posed sufficient hydrostatic pressure to overcome sur tension forces, and to ensure uniform contact fr instant of melting. In each case the assembly was h for a few seconds to 400—500°C to complete the all ing process.

Figure 1 **Typical "long" specimen of GaAs.** *Each division of the scale below the specimen represents 1 mm.*

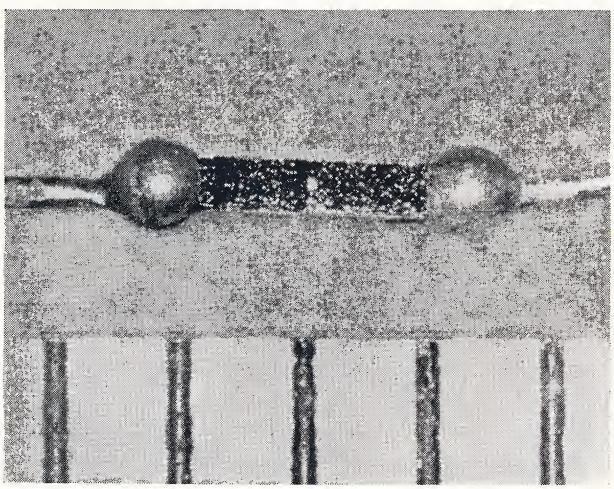

Figure 2a **Typical "short" specimen of Ga fore alloying.**

Figure 2b **Typical "short" specimen of GaAs after alloying.**

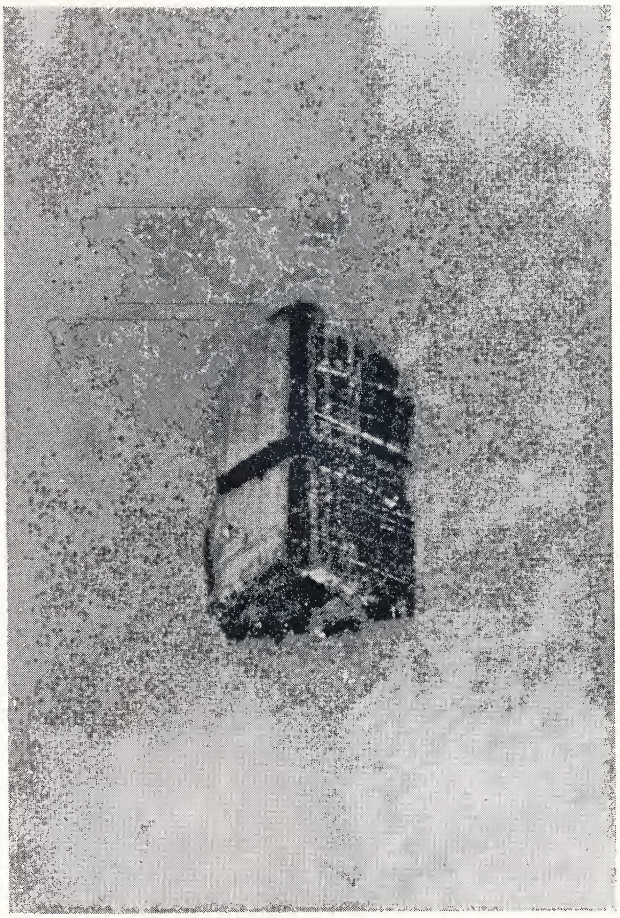

Figure 2c **Typical "short" specimen of GaAs after grinding.**

...chief problems encountered arose from the difficulty ...hieving wetting by, and the large contact angle of ...on Sn on GaAs. Although the special design for the ...hite molds helped considerably, it was found necessary ...take precautions to prevent the formation of a thin but highly tenacious layer of Ga_2O_3, whose presence prevents wetting at low temperature. These included the use of unusually pure forming gas as a protective atmosphere and the removal of all traces of adsorbed water from the ...s and the mold. Both were dried in a vacuum dessi... ...diately before use, and the empty mold was ... a high temperature in forming gas. The gas was ...d by chemical drying, then by passing over heated ...urnings to ensure the complete reaction of oxygen, ...urther chemical drying, and finally by drying ...iquid nitrogen trap. In addition, the Sn spheres ...e cleaned of surface contamination by firing on a graph... ...p in forming gas to over 1000 °C.

...further difficulty arose from the "thermal conversion" ...the *n*-type GaAs, which was apparently due to the rapid diffusion of copper (an acceptor). This was overcome by a combination of NaCN rinses, extreme cleanliness in handling, and low alloying temperature. For other combinations of materials, the techniques described were used without significant modifications.

• *2.3 Electrical connections and encapsulation*

For the long bar specimens, electrical connection was made simply by soldering fine copper wires to the Sn contacts (Fig. 1). For the short specimens, this was not suitable because the inductance so introduced would have a reactance, at the frequencies of interest, that would obscure the properties of the specimen itself. These specimens, which after alloying had the form shown in Fig. 2b, were therefore modified to permit them to be connected in various circuits while introducing the very minimum of inductance. The circular cross-section of the semiconductor-metal sandwich was first reduced to a triangular shape (Fig. 2c) by grinding on abrasive paper. The resulting prism was next laid on its side on the flat bottom of a shallow cylindrical mold which was then filled with epoxy resin. After the resin had hardened, it was removed

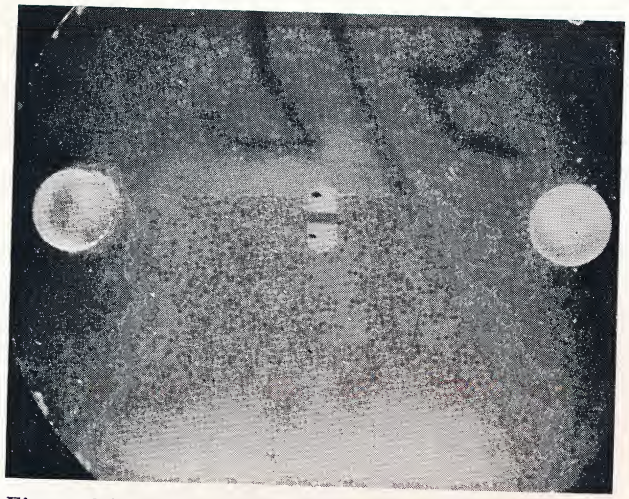

Figure 2d **Typical "short" specimen of GaAs after encapsulation.**

from the mold and the specimen was exposed by further grinding. The two holes shown in Fig. 2d were then drilled in the disc of resin in precise relationship to the exposed metal electrodes. Connection to the specimen could then be made by small leaf springs guided into contact with the electrodes by pins engaging the holes. Finally, the cross section of the specimen was adjusted to the desired value by additional grinding of the exposed face, and its dimensions were estimated from optical measurements of this face and the known angles of the prism.

The specimens normally were not etched after alloying; the electrical properties to be discussed appeared to be independent of surface condition, and etching would have introduced a considerable risk of undercutting the semiconductor near the contacts.

• *2.4 Electrical measurements*

All experiments except those described in Section 3.2.4 were made at room temperature. Certain preliminary measurements were made on each specimen. The "ohmic" nature (at low fields) of the contacts was checked by examining the linearity of its current-voltage characteristc with a conventional curve tracer; the few nonlinear specimens found were rejected. The low-voltage resistance of the specimen was then measured by means of a 1 kc/sec bridge, and the apparent resistivity of the semiconductor was computed from this value and its previously measured dimensions.

In experiments involving the application of strong electric fields to the semiconductor, it was necessary, in order to avoid overheating and other damage to the specimen, to apply this field in the form of short pulses of low duty cycle. Most of the work was performed with pulses of between 0.5 and 30 nanoseconds duration at a repetition rate of 120 sec^{-1}, which were obtained by charging a length of coaxial transmission line to a high voltage and discharging it into a 50 ohm output cable by means of a coaxially mounted mercury wetted-contact relay. The coaxial mounting was arranged to minimize the impedance mismatch presented to the pulse. For some purposes, pulses with nonrectangular shapes were generated by means of special combinations of charged transmission lines. When longer pulses with higher repetition rate were needed, they were obtained from a commercial vacuum-tube pulse generator.

In order to measure the current through the specimen while a known pulse voltage relatively independent of current was applied to it, it was connected in the fixture shown in Fig. 3a. The shunt resistor R_1 served to reduce the impedance of the pulse source to a low value, while R_2 developed a voltage which was proportional to the current and much less than that across the specimen.

In the equivalent circuit of Fig. 3b, the element L represents the unavoidable stray inductance of the connections between R_1, R_2, and the specimen. As a result of the effective screening provided by the fixture, and of the small length/diameter ratio adopted for the resistor R_2, the component of output voltage that was due to inductive coupling with the specimen current was reduced to a negligible value; thus the mutual impedance between specimen and output circuits remained purely resistive up to the highest frequencies observable. The resistors R_1 and R_2 normally had values of 1 or 2 ohms, but values up to 15 ohms were used occasionally to obtain higher specimen voltages or greater current sensitivity. The quantity $L/(R_1 + R_2)$ was estimated by measuring the time constant of the circuit when the specimen was replaced by a metal dummy. In this way the value of L was found to be about 2×10^{-9} H. Since the resistance of actual specimens generally fell in the range 20-200 ohms, the L/R time constant existing during experiments was from 10^{-10} to 10^{-11} sec.

Measurements on the current waveform were made either oscillographically or by spectrum analysis. When successive pulses were identical, or nearly so, a Tektronix 661-4S2-5T1 sampling oscilloscope with a rise time of less than 10^{-10} sec was used. For waveforms with Fourier components of interest below 1 Gc/sec and with sufficient amplitudes, a Tektronix 519 travelling-wave oscilloscope could be used, even if there were random differences between successive pulses. Studies of the components above 1 Gc/sec of such pulses and all measurements of frequency were made with a wide-range spectrum analyzer employing a sweep oscillator of appropriate frequency range as the local oscillator for a broad-band crystal mixer. The output of the mixer was amplified and detected by a conventional 200 Mc/sec i.f. amplifier; the video output from this was fed to the vertical channel of a conventional oscilloscope whose horizontal deflection

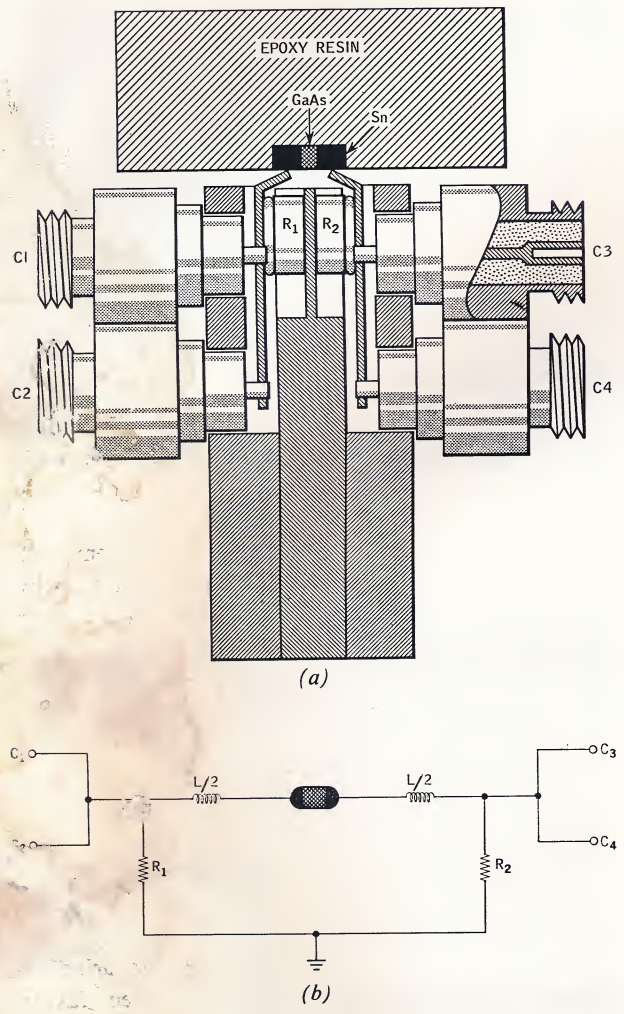

Figure 3 **(a) A cross-sectional view of the fixture used for measurement of current waveforms; (b) equivalent circuit for the fixture.**
C_1, C_2, C_3, and C_4 are, respectively, the pulse input terminal, the voltage waveform connection, the current waveform connection, and the lead to the spectrum analyzer.

was derived from the sweep oscillator. Arrangements were made to switch on the oscilloscope spot only for a fraction of a microsecond following the application of a voltage pulse to the specimen, thus preventing the masking of the desired signal by light scattered from the vertically undeflected oscilloscope spot during the intervals between pulses. Components of the input pulse at the intermediate frequency were eliminated by means of a high-pass filter inserted between the specimen and the mixer. With this system, the frequency spectrum of pulses as short as 10 nanoseconds could be displayed over the whole of any one of the ranges 0.25-1, 1-2, 2-4, and 4-8 Gc/sec. Frequency measurements were made by comparison with calibrated signal generators.

The pulse voltage across the specimen was found by measuring the total voltage across the specimen and R_2, and subtracting the small current-measuring voltage existing across R_2 alone. Absolute measurements of the various pulse amplitudes were made by comparison against a dc potentiometer, using the travelling-wave oscilloscope only as a null indicator. A direct display of pulsed current-voltage characteristics (not corrected for voltage across R_2) was made by sampling simultaneously the current waveform with the A channel of the two-channel 4S2 sampling unit and the voltage with the B channel. This yielded a deflected spot whose coordinates were proportional to the current and voltage existing during an interval of less than 10^{-10} sec starting after a fixed delay from the beginning of the applied pulse.* This delay was chosen so that small, but unavoidable, transients due to transmission-line discontinuities, etc., had died away. The amplitude of the voltage pulse applied to the specimen was varied by a variable attenuator which was motor-driven during photographic recording. The synchronizing pulse for the sampling oscilloscope was derived from a point before the attenuator, so that its amplitude remained constant while the specimen voltage varied. This eliminated errors due to the small dependence of sampling delay on synchronizing pulse amplitude.

3 Results

• *3.1 Primary phenomenon*

3.1.1 Current-voltage characteristics

The nature of the current instability that has been observed can best be illustrated by the sampled current-voltage characteristics shown in Fig. 4. Mathematically, these are plots of current as a function of voltage with time held constant (see Section 2.4). The relationship between I and V near the origin is symmetrical and nearly linear, in keeping with the idea that no rectifying junctions are present. The behaviour at higher voltages is qualitatively similar for all lengths of specimen. As the voltage is increased, the dc conductance first decreases slightly, presumably as a result of changes in electron mobility; then, at some particular value of voltage (the threshold V_T), there occur wide differences in current between successive samples. This appears as a large scatter of the dots representing individual samples, but the instantaneous value of the fluctuating current at voltages above V_T

* A temporary modification is needed in the 5T1 timing unit used for this display; unless the lead from pin 11 on plug P4 is disconnected, the sampling delay is proportional to horizontal deflection and entirely spurious results are obtained.

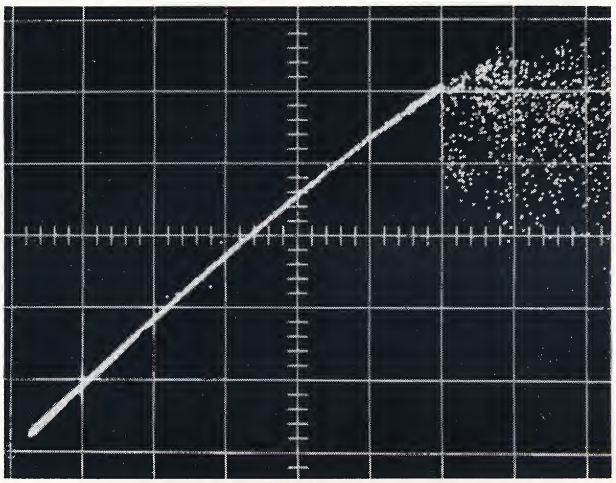

(*a*)

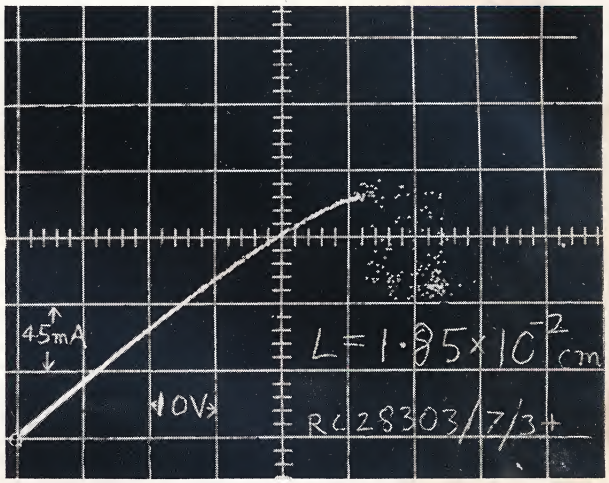

(*b*)

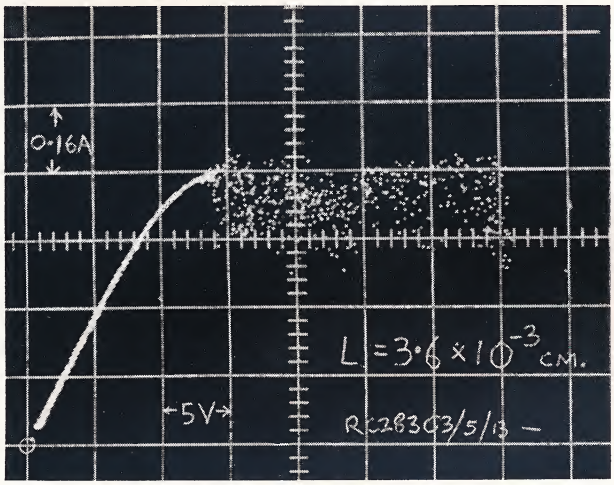

(*c*)

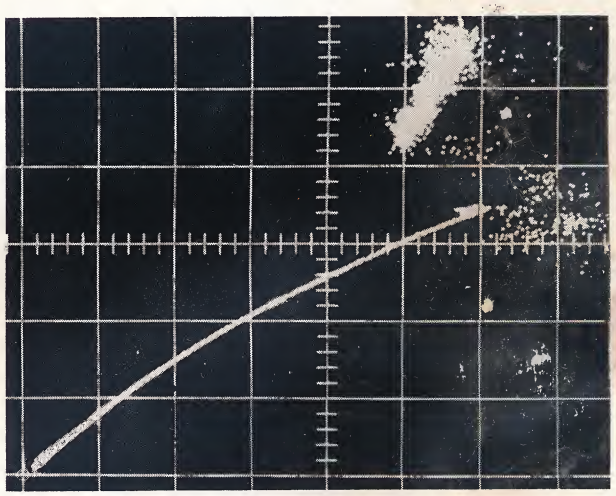

(*d*)

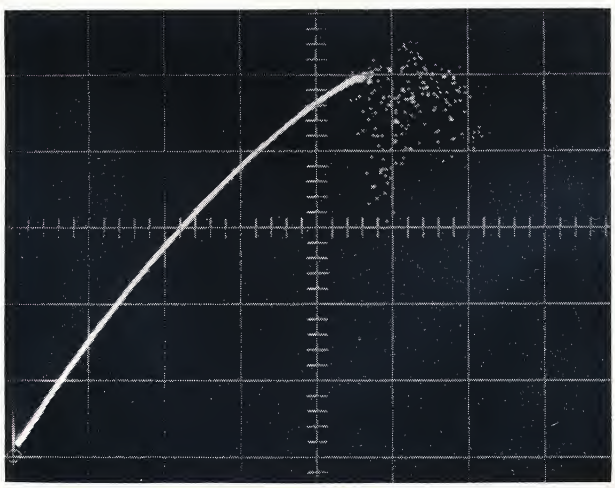

(*e*)

Figure 4 **Sampled current-voltage characteristics of typical n-type GaAs and InP specimens.** *Materials, lengths, and approximate vertical and horizontal sensitivities (VS and HS) per major division are as follows:*

(*a*) *GaAs, L = 9.2 × 10⁻² cm, VS = 0.0 30V;*

(*b*) *GaAs, L = 1.85 × 10⁻² cm, VS = 45mA, HS = 10V;*

(*c*) *GaAs, L = 3.6 × 10⁻³ cm, VS = 0.16A, HS = 5V;*

(*d*) *InP, with In-Te non-injecting contacts and threshold behavior as in Fig. 8b, L = 1.35 × 10⁻² cm, VS = 1.2A, HS = 16V;*

(*e*) *InP with Sn-Te contacts showing injection above threshold as in Fig. 8a, L = 7.7 × 10⁻³ cm, VS = 0.75A, and HS = 10V.*

rarely exceeds its value I_T at V_T. Consequently, the time-average value decreases as V passes through V_T. This gives rise to a low-frequency negative resistance, which can cause relaxation oscillations or bistable behaviour if the inductance or resistance of the external circuit is too great. It is chiefly for this reason that the external impedance was kept low in making these measurements. The results shown for GaAs are quite typical of those obtained from a large number of specimens. Even between supposedly identical specimens, or indeed between the same specimen in its two possible polarities, there often exist differences of detailed behaviour, however. For example, there are variations of the order of 5% in the ratio of dc conductance at V_T to dc conductance at zero voltage, as well as the scatter in V_T discussed in the next section. These differences are ascribed to variations of conductivity in different parts of the specimen, inherited from the inhomogeneous crystals used. Only occasionally was a specimen found in which the current continued to increase above V_T, but in no case has an ohmic-*n*-ohmic structure failed to show instabilities of current. The differential conductance $\partial I/\partial V$ always decreases as the threshold is approached, but only in the very shortest specimens does its value there fall to approximately zero (Fig. 4c). In *p*-type GaAs, with ohmic contacts made using In, no instabilities have been observed up to fields of about 4×10^4 V cm^{-1}.

The current-voltage characteristics of short *n*-type InP specimens with non-injecting contacts (Fig. 4d) are often quite similar to those of GaAs; with injecting contacts, a more complicated behaviour is observed, as is shown in Fig. 4e and discussed in Section 3.1.3.

3.1.2 Threshold conditions

The threshold voltage V_T, which is by definition the applied voltage at which the current first shows instability, is generally quite sharply defined. Values were obtained for a number of specimens, each pulsed in both possible polarities. The two values of V_T for a given specimen were usually fairly close, but agreement to nearer than 10% was relatively uncommon. There was also considerable scatter of V_T among similar specimens. The results for GaAs are shown in Figure 5a, in which V_T is plotted against the length L of the specimen between the plane Sn contacts. It is apparent that V_T increases as L does, but not exactly in proportion; on the log-log plot shown, the slope is clearly not unity but is approximately equal to 0.8. This means that the average value of E_T, the electric field at threshold, is not constant but varies from about 1250 V cm^{-1} in the longest to about 3700 V cm^{-1} in the shortest specimens used. Some data for InP are shown in Fig. 5b.

The drift velocity v_T at threshold can be estimated for GaAs as follows. The zero-field mobility $\mu(0)$ is known

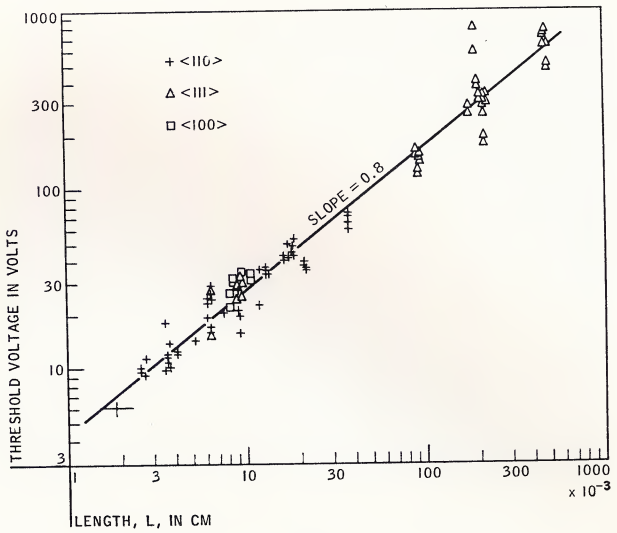

(a)

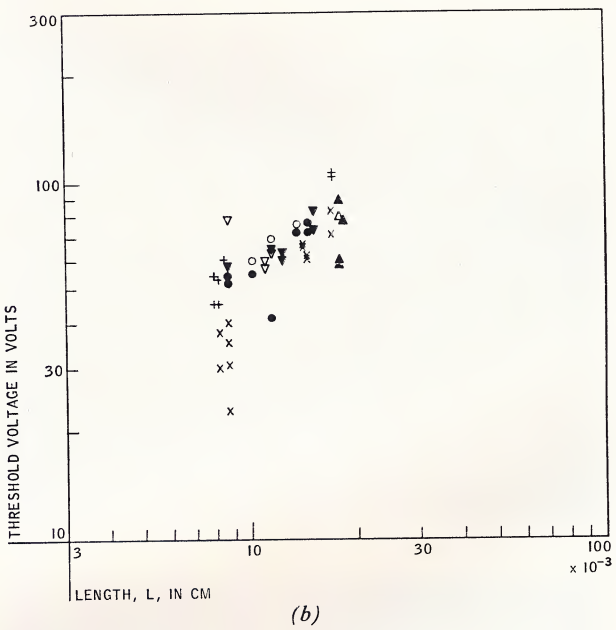

(b)

Figure 5 **The dependence of threshold voltage V_T on specimen length L.**
Fig. 5a applies to n-GaAs crystal RC 28303; data for crystal G-133 fall within the scatter of the points shown. The solid line illustrates the trend of the data; the various symbols indicate the direction of current flow in the crystal. Fig. 5b applies to n-InP crystals InP-2 and InP-4, with the shapes of symbols denoting the contact material: + denotes Sn; ×, In; △, In-Ge; ○, In-Te; and ▽, In-Se. Open symbols and crosses indicate injecting threshold (as in Fig. 8a); solid symbols indicate oscillating behaviour (as in Fig. 8b.)

(5000 cm^2 V sec^{-1}), as is the smoothed value of $E_T(L)$ from the line drawn in Fig. 5a. Typical values of the ratio $\mu(E_T)/\mu(0)$ are also known from *I-V* data, on the assumption that the number of electrons does not change, being about 0.88 at $L = 1.85 \times 10^{-2}$ cm and 0.78 at $L = 2.5 \times 10^{-3}$ cm. The threshold drift velocity is then given by $v_T = \mu(0)\{\mu(E_T)/\mu(0)\}E_T$. Values calculated in this way are 0.94×10^7 cm sec^{-1} at $L = 1.9 \times 10^{-2}$ cm, and 1.44×10^7 cm sec^{-1} at $L = 2.5 \times 10^{-3}$ cm.

3.1.3 Time-dependence of current

Further information about the instability can be obtained by plotting current as a function of time, with voltage fixed, as a conventional oscilloscope trace. Figure 6 shows some examples which are believed to be typical of *n*-type GaAs. The results for a long specimen are shown in Fig. 6a as a trace obtained with the travelling-wave oscilloscope. Behaviour which is apparently identical with that shown

Figure 6 **Waveforms of current through n-type GaAs specimens from crystal RC 28303.**

The driving signal is applied by the low impedance circuit of Fig. 3 so that the voltage across the specimen remains nearly constant during the pulse. Each photograph is a double exposure showing the current waveform when the voltage is both just less and just greater than the threshold value. Except in the expanded view of Fig. 6d the time scale is 2 nsec per major division. Lengths and vertical scales (VS) per major division are as follows:

(a) $L = 9.2 \times 10^{-2}$ *cm, VS = 1.5A;*
(b) $L = 1.9 \times 10^{-2}$ *cm, VS = 0.9A;*
(c) $L = 6.1 \times 10^{-3}$ *cm, VS = 45mA;*
(d) $L = 2.5 \times 10^{-3}$ *cm, VS = 0.23A. The time scale in the expanded view (above) is approximately 0.2 nsec per division.*

(a)

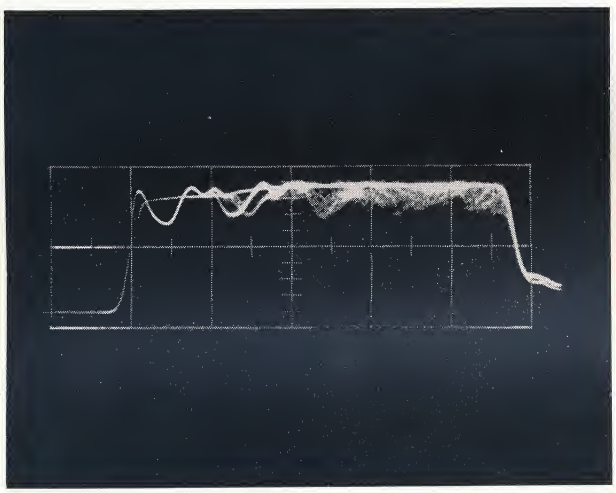

(b)

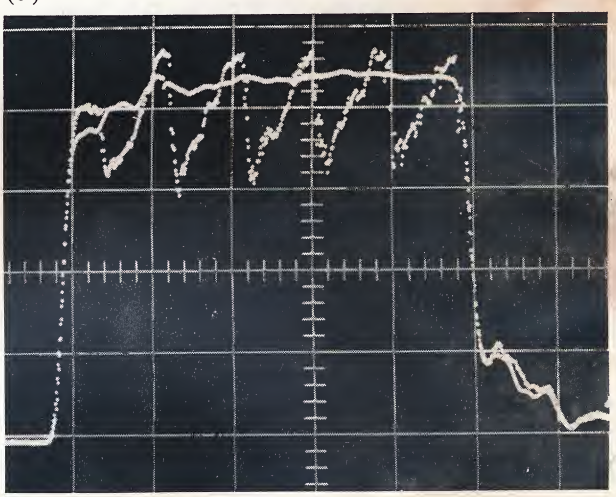

(c)

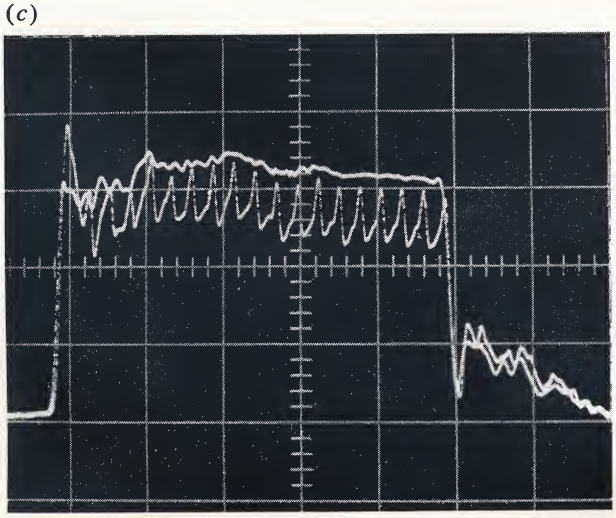

(d)

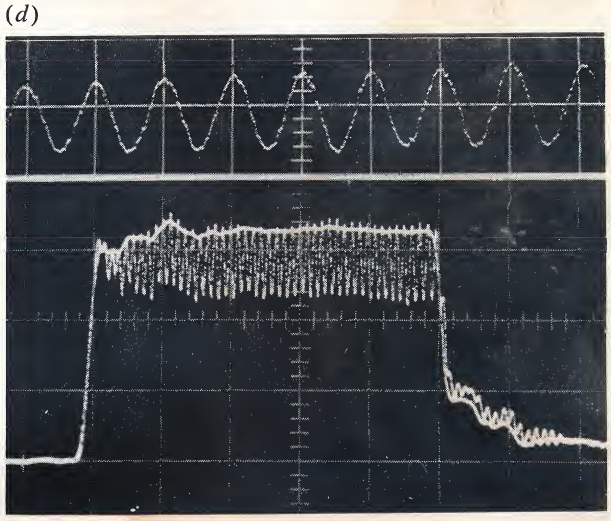

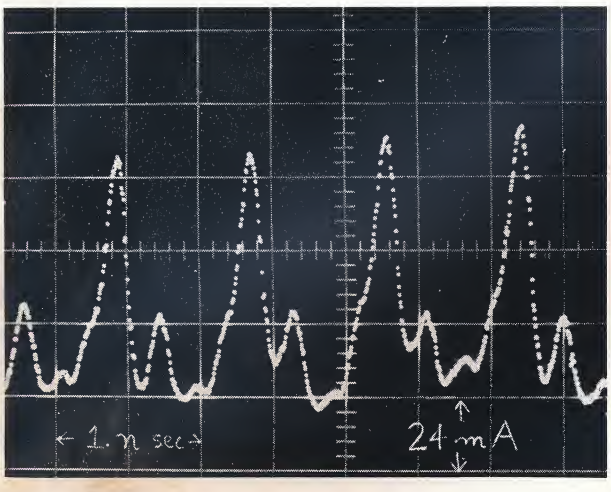

Figure 7 **An extreme example of a non-sinusoidal waveform.**
The material is n-type GaAs from crystal RC 28303 and the length is 9.4 × 10^{-3}cm. Vertical and horizontal scales are, respectively, 24 mA and 0.5 nsec per major division.

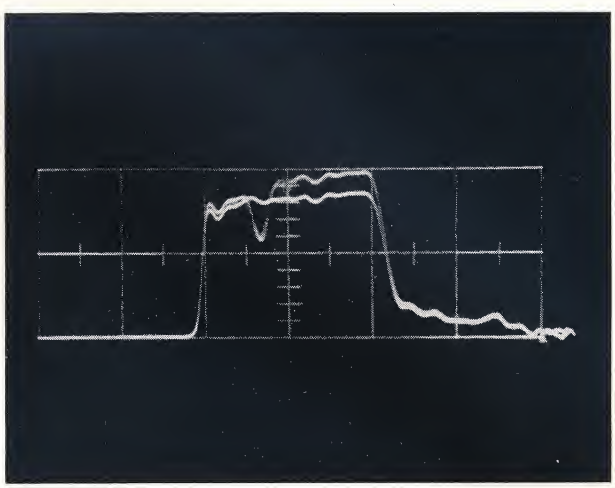

Figure 8a **Current waveform for specimen of n-type InP crystal InP-4.**
Photograph is multiple exposure, as in Fig. 6. Specimen length (L) is 7.9 × 10^{-3} cm, contacts are Sn, the time scale (TS) is 2 nsec per major division and the vertical scale (VS) is 1.65 A per major division.

(except of course for the actual value of V_T) was obtained for specimens from crystal RC28303 of all lengths studied from 0.1 to 0.5 cm, as well as for specimens of similar length from crystal 52-26. Long specimens from crystal G133 were not examined. Like all the other illustrations in Fig. 6, Fig. 6a is a multiple exposure; the rectangular pulse shows the variation, I_T, of current with time when V is just less than V_T, whereas the waveforms varying randomly in time are the record of a number of successive pulses at a fixed value of V somewhat greater than V_T. Under the latter circumstances, there occurs at the beginning of each pulse a sudden decrease in current, followed by a number of fluctuations to a value usually not greater than I_T. At first these fluctuations are relatively regular, and coherent from pulse to pulse, but near the end of the 10-nanosecond pulse all correlation is lost, and the waveform resembles random noise. Spectrum analysis shows that the spectral intensity is roughly constant at low frequencies, dropping off at about 2 Gc/sec. Consequently, not much detail is lost because of the limited frequency response (1 Gc/sec) of the oscilloscope.

For specimens of length about 2×10^{-2} cm and shorter, the current fluctuation takes the form of an oscillation of well-defined period whose phase remains substantially constant during the pulse (*intra-pulse* coherence). In most of these specimens, however, the phase relative to the applied voltage pulse fluctuates randomly from one pulse to the next. As the frequency of oscillation is generally above the cutoff frequency of the travelling-wave oscilloscope, only a sampling oscilloscope would have a sufficiently fast response, but the lack of *inter-pulse* coherence prevents such an oscilloscope from giving a meaningful display. In a few specimens there is good inter-pulse coherence for certain values of voltage; some waveforms of this type are shown in Figs. 6b, 6c, and 6d. In these cases also, the instantaneous value of current does not significantly exceed I_T, which is shown superimposed. It will be noted that as the length of specimen is decreased, the frequency of oscillation increases and the waveform appears to become more nearly sinusoidal. It is not known whether this latter effect is due to a possible failure of the sampling oscilloscope to respond to the progressively higher frequencies involved. No great significance should be attached to the exact shapes of the waveforms shown in Figures 6b and 6c; waveforms vary greatly between specimens, as is illustrated by comparing those two and that shown in Fig. 7. Whilst all the waveforms shown are for specimens from crystal RC28303, indistinguishable results were obtained with crystal G-133.

Specimens of *n*-type InP with contacts containing Sn also show a time-dependent current above a threshold voltage V_T (Fig. 8a) but its nature is very different from that discussed above. Although the same sudden decrease of current occurs, it is always followed within a fraction of a nanosecond by a jump to a value rather greater than I_T. The corresponding current-voltage characteristic is shown in Fig. 4e. Experiments with two-level voltage pulses, in which an initial portion with amplitude greater than V_T is followed by a long "back porch" of amplitude less than V_T, show that this increase in conductance persists at lower voltages and dies out only after several tens of nanoseconds. It is assumed that this

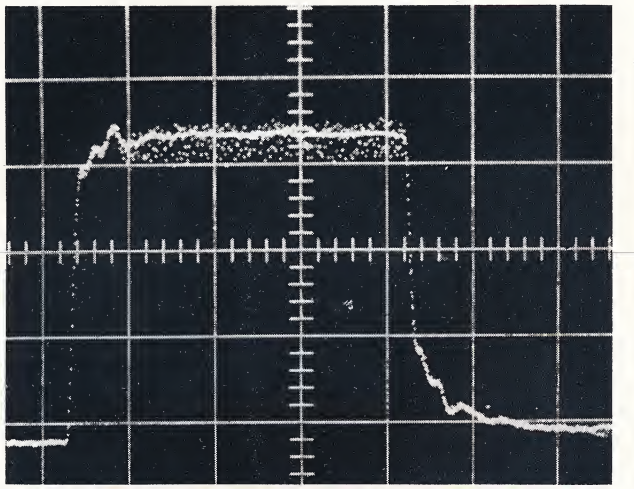

Figure 8b **Current waveform for specimen of n-type InP crystal InP-4.**
Photograph is multiple exposure, as in Fig. 6. Specimen length (L) is 7.5 × 10^{-3} cm, contacts are In, the time scale (TS) is 5 nsec per major division and the vertical scale (VS) is 0.45 A per major division. The solid trace represents the current at a voltage just less than V_T; the dots are the sampling oscilloscope's response to an oscillatory waveform (at an applied voltage above V_T) lacking coherence.

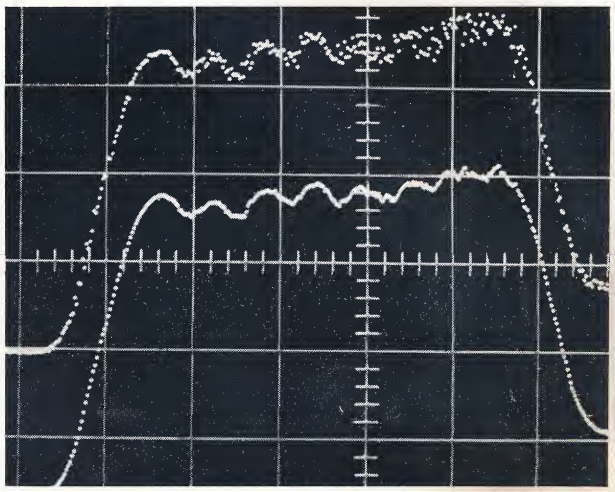

Figure 8c **Current waveform for specimen of n-type InP crystal InP-4.**
This view represents partially coherent oscillations (frequency = 2.8 Gc/sec) for the same specimen and vertical sensitivities as in (b). The unsmoothed display is shown above the smoothed display. TS = 0.5 nsec per major division.

results from the imperfectly "ohmic" nature of Sn alloy contacts on *n*-InP, which probably become hole-injecting at high electric fields. On this assumption, the transition to the high-current, low-voltage state (Fig. 4e) can be understood as an example of avalanche injection.[11] When In is substituted for Sn, this effect occurs less frequently, and in many specimens the current does not increase much above I_T, just as is the case for *n*-GaAs. Contacts of In-Te, In-Se, or In-Ge reduce its incidence even further; this comparison is shown in Fig. 8b. The degree of intrapulse coherence is, however, much less than for comparable specimens of GaAs, and in only one case was it possible to observe an oscillation which was coherent for even a few cycles. This waveform is shown in Fig. 8c. The "smoothed" display is one in which each point represents the average of a number of sampling operations, so that the scatter is decreased and the oscillations are made more clearly visible. In the "unsmoothed" display the progressive loss of coherence can be seen. In all cases where oscillations were observed, they persisted with undiminished amplitude for at least 0.5 microsecond, which is the length of the longest pulses used.

3.1.4 Frequency spectrum of current

For the majority of cases, the high frequency of oscillation combines with the lack of interpulse coherence to make it impossible to measure the period oscillographically. However, spectrum analysis does give a definite result for these specimens. The degree of purity of the spectrum varies somewhat from specimen to specimen, but in only one or two cases have short *n*-GaAs specimens been found for which a frequency of oscillation could not

Figure 9 **Typical frequency spectrum of current through n-type GaAs specimen.**
The length of the specimen is 1.29 × 10^{-2} cm and the duration of the applied voltage pulse is 40 nsec. The frequency scale is 20 Mc/sec per major division and the center frequency is 1.29 Gc/sec.

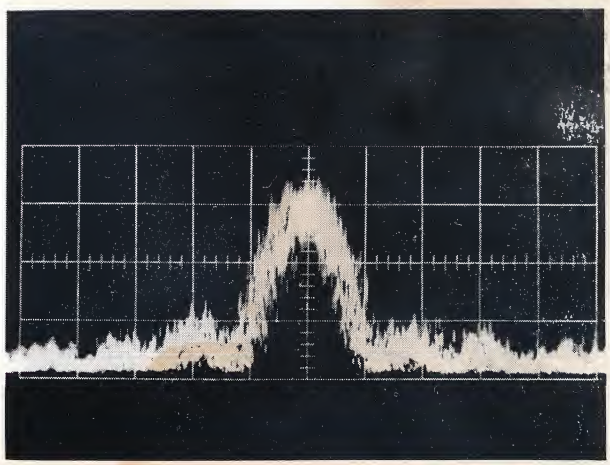

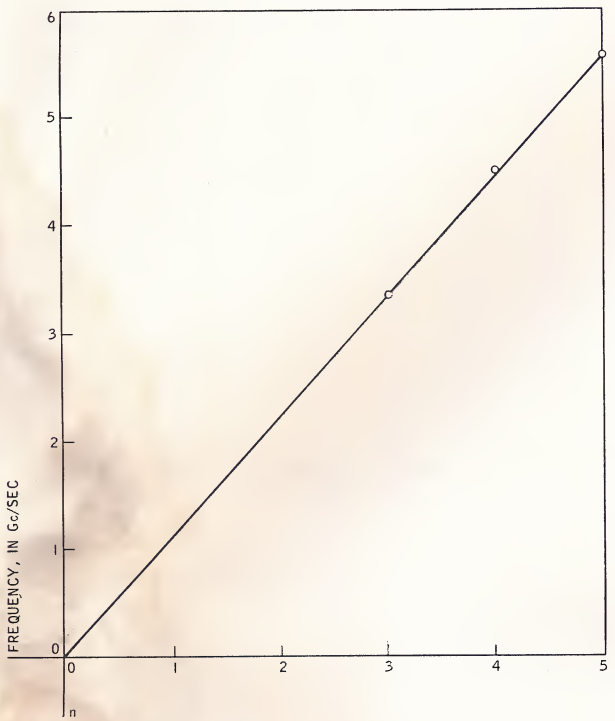

Figure 10 **Example of assignment of "harmonic" numbers. The period deduced from the data shown is $(1.12\text{Gc/sec})^{-1}$.**

be defined within 10 to 20 Mc/sec; generally, the uncertainty is much less than this (Fig. 9). A disadvantage of the spectrum analysis technique is that it is not possible to tell from a single measurement whether the lowest frequency observed is equal to the reciprocal of the period. In those cases where comparison with an oscillographically determined period is possible, the lowest frequency generally corresponds to it. Such results give a few unambiguous points on a graph of "fundamental" frequency (τ^{-1}) versus specimen length; for other specimens, the following procedure was adopted.

A search was carried out over the various frequency ranges of the spectrum analyser, with the specimen voltage adjusted to the lowest value at which clearly defined frequency components were visible in that range; this generally was a value somewhat greater than V_T. For most specimens, the observed frequencies increased slightly but measurably as the voltage was increased, and in one or two cases the rate of increase was as strong as proportional to voltage. The measured frequencies f were then divided by a small integer n which was chosen to give as little scatter as possible when these points together with those obtained from measurable periods were plotted on a log-log graph against length L. There was generally no ambiguity about the values of n to be chosen. The values used did not always form an unbroken sequence starting with unity; often certain "harmonics" were absent, as sometimes was the "fundamental" $n = 1$. The case illustrated in Fig. 10 demonstrates this point. Here the frequencies 3.35, 4.50, and 5.57 Gc/sec clearly correspond to $n = 3, 4, 5$ of a series for which the components with $n = 1, 2$ are undetectably small. Nonetheless, the absent "fundamental" 1.12 Gc/sec is well defined. Values of f/n obtained in this way are shown in Fig. 11. Because of the way in which the data were taken, different frequency components from a particular specimen do not always give exactly the same value of f/n and, moreover, the frequencies were often slightly different for the two directions of current flow. Consequently, in Fig. 11, most of the specimens are represented by several points.

The existence of strong frequency components for large values of n means that the current waveform must be very non-sinusoidal. This is borne out by cases such as those shown in Figs. 6b, 6c, and 7, where the time-variation of current can be resolved.

The line in Fig. 11 is drawn to interpolate between values of frequency calculated for $L = 2.5 \times 10^{-3}$ cm and $L = 1.9 \times 10^{-2}$ cm. The calculated frequencies are

Figure 11 **Relationship between "fundamental" frequency of oscillation (see text, Section 3.1.4) and length of n-type GaAs specimens from Crystal RC 28303.**
Crystal orientations shown represent direction of current flow. The line is drawn to interpolate between the frequencies, calculated for lengths of 1.9×10^{-2} cm and 2.5×10^{-3} cm on the assumption that the period of oscillation is equal to the transit time of electrons at the threshold voltage.

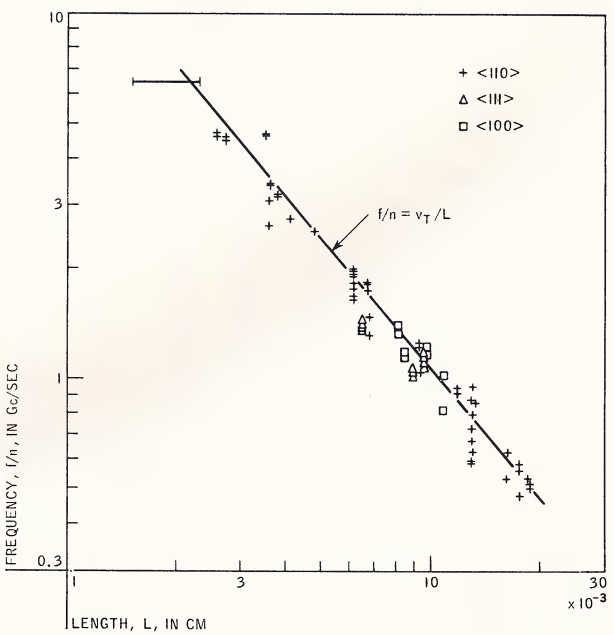

those which correspond to a period equal to the transit time of electrons between the electrodes; this time is derived from the value of L and v_T, the drift velocity at threshold, which is estimated as described in Section 3.1.2. The close agreement between this line and the experimental points shows quite clearly that the period of oscillation is equal to the transit time. The reason that the slope of the line is -1.2 and not -1.0 is that v_T is a function of L, as a result of changes in both $\mu(E_T)$ and E_T, and so the transit time is not quite inversely proportional to length.

A coherent oscillation has so far been observed in only one specimen of InP (Fig. 8c). The frequency of 2830 Mc/sec was somewhat ill defined because of poor coherence; the corresponding period is equal to approximately one-half of the estimated transit time. From this one case it is not possible to deduce whether the relation between frequency and transit time observed for GaAs is invalid for InP, or whether this is another case of the component $n = 1$ being missing. The result does show, however, that the phenomenon of coherent microwave oscillation of current is not confined to GaAs.

• *3.2 Diagnostic experiments*

Various additional experiments were performed in an attempt to distinguish between mechanisms which might cause the phenomena described above. As the results of most of them were negative, they are discussed only briefly here.

3.2.1 Contact vs bulk phenomena

That the initiation of current instability is a bulk effect, and is independent of contact conditions, was deduced in two ways. First, no systematic difference could be observed between "long" GaAs specimens having contacts made by alloying Sn, and those having mechanical pressure contacts of In. The pressure contacts were, however, nonlinear and of very high resistance at low voltages. In InP, moreover, even though two very different types of instability could be observed, depending partly on the contact material used, no correlation with the threshold field was found (Fig. 5b). Second, two specimens of GaAs approximately 1 mm long, with Sn contacts, were modified by cutting a slot about 0.1 mm wide, normal to the direction of current flow, and midway between the contacts. The threshold voltage was measured repeatedly as the slot was deepened. The results are plotted in Fig. 12, in which the zero-field dc resistance R_0 is used as a measure of slot depth. If the phenomenon were associated with the contacts, the threshold current density and electric field *at the contacts* should remain constant. Since their area does not change, the threshold current should not, and V_T should then be proportional to R_0. On the other hand, the progressive concentration of electric field around the bottom of the slot means that a given maximum field in the bulk is reached at lower voltages as the resistance rises. Thus, for a bulk effect, V_T should decrease as R_0 increases, as is observed.

3.2.2 Persistence effects

Several experiments were performed in which the current through a GaAs specimen at time t_2 was measured at some voltage below threshold, while the voltage at some preceding time t_1 was varied above and below threshold. Because of limitations imposed by inductance and oscilloscope response time, $t_2 - t_1$ could not be made less than about 0.5 nanosecond. Outside of this interval, however, there was never observed any persistence of the conductance changes produced by driving the specimen beyond threshold.

The behavior of InP specimens under the same circumstances was discussed in Section 3.1.3.

3.2.3 The effect of a magnetic field

A magnetic field of 3300 gauss, applied either parallel or normal to the direction of current flow, had a very small effect on V_T in long and short specimens, and on the frequency of oscillation in short specimens. These effects were of the same order as the zero-voltage magnetoresistance.

3.2.4 The effect of temperature

For a long GaAs specimen, the effect of varying the temperature between 300° and 77°K was to decrease the threshold voltage by a factor of about 2. The threshold current, however, decreased much less, remaining practically constant over most of the range before finally decreasing, at 77°K, to about 70% of its room temperature value. The carrier concentration in the material used is

Figure 12 **Dependence of threshold voltage on slot depth in field-concentration experiments.** (*See text, Section 3.2.1*). *The zero-field resistance R_0 is used as a measure of slot depth.*

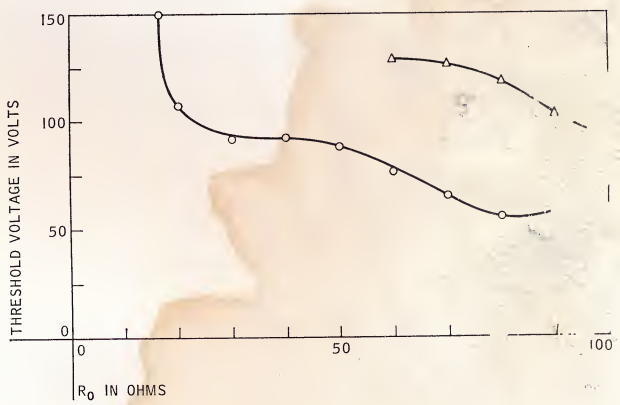

thought to change in a roughly similar way. Although more data are needed, it is concluded that the drift velocity at threshold is probably nearly independent of temperature.

3.2.5 The effect of specimen cross section

Changes of cross-sectional dimensions were found to have no influence (larger than the scatter between supposedly identical GaAs specimens) on either threshold voltage or frequency of oscillation. This was true whether the comparison was between different specimens or, as shown in Table 2, between measurements made on the same specimen ground to different thicknesses. Since, in this last case, the impedance Z presented by the external circuit remained nearly constant and equal to $3\Omega + j20\Omega$, these results can also be interpreted as showing that changing the ratio Z/R_0 has no noticeable effect on V_T.

Table 2 **The effect of changes in cross-sectional area on threshold voltage V_T and oscillation frequency f for a specimen from GaAs crystal RC 28303.** *Specimen length remains constant at 1.3×10^{-2} cm. The cross-sectional area is calculated from the zero-voltage resistance R_0.*

R_0 *in ohms*	*Area in* cm^2	V_T *in volts*	*f in Mc/sec*
41.6	4.5×10^{-4}	36.8	1290
206	9.1×10^{-5}	36.4	1550
405	4.6×10^{-5}	37.3	1430

3.2.6 The effect of external circuit impedance

The measurements of oscillation frequency discussed in Section 3.1.4 were made under circumstances where the resistance, and in most cases the inductive reactance, of the external circuit was much less than the zero-voltage specimen resistance R_0. At the very highest frequencies, the external reactance was in some cases comparable with, but still less than, R_0. To examine the effect of external reactance, a specimen of GaAs with $R_0 = 64\Omega$ was connected so that the external impedance consisted of $50\Omega + j0$ shunted by a variable, open-ended length of transmission line. Thus the impedance could be varied as the length of line was altered over a range including 0, 50Ω, and $100 \pm j100\Omega$. The frequency of oscillation varied over the range 2175 to 2550 Mc/sec as the length was altered. In certain other experiments described in Section 4, in which specimens were connected to a high-Q coaxial cavity, a similarly small tuning range was observed for most specimens. In one case, however, coherent oscillation over a 2:1 frequency range was observed.

3.2.7 Radiofrequency impedance below threshold

The rf reflection coefficient of a GaAs specimen was measured during the time that a voltage pulse 0.5 μsec long, and of amplitude just less than V_T, was applied. The impedance was found to be somewhat greater than in the absence of the pulse, partly because of the decrease in mobility produced by the high field, and partly because of heating produced by the long pulse. No singularities of impedance as a function of frequency were found, even at those frequencies at which oscillation was observed when the voltage was increased above V_T.

3.2.8 Optical and surface effects

No difference was found between GaAs specimens with ground surfaces and those whose surfaces had been etched. Intense steady illumination of the GaAs during operation was also without effect. A search for radiation was made, from the visible spectrum out to about 55μ, by the use of a silicon solar cell and of a vacuum thermocouple with a CsBr window; each was mounted as close as possible to the GaAs specimen. The pulse repetition rate was reduced to 13 c/sec, and the 13 c/sec component of the detector voltage was amplified and phase-sensitively rectified. The only radiation detected was found, by the use of filters, to have a maximum near 10μ, which is the peak of the spectrum of a black body at 300°K. Since the intensity of this radiation increased when the specimen was covered with colloidal graphite, it is deduced that its origin is thermal and that it is due to modulation of the specimen temperature by the 13 c/sec component of the power input.

4 Applications

Since the phenomenon under investigation involves the transformation of pulse current directly into microwave power, it is natural to enquire whether useful technological applications exist. The answer to this question depends, among other things, on the absolute level of the available rf power and on the efficiency of conversion. To measure these quantities under optimum conditions, a coaxial cavity resonator of adjustable length was constructed, in which various GaAs specimens were connected between the inner conductor of the cavity and a metal disc closing the open end of the cavity. The disc was insulated from the body of the cavity by a thin sheet of dielectric, which provided a capacitance to ground of approximately 700 pF. The other end of the cavity was short-circuited by a movable plunger, so that a pulse voltage applied between the disc and ground appeared across the specimen, but the large capacitance prevented any significant rf voltage from being developed across the pulse generator. Power was coupled out of the cavity by a rotatable loop connected through a length of coaxial cable to a 50 ohm load. Only those specimens whose resistance was relatively high could

be matched satisfactorily in this way; with lower resistance specimens, optimum matching was not possible, and in many cases the rf amplitude became unsteady and jumps of oscillation frequency occurred. A cavity constructed of coaxial line with a lower characteristic impedance would probably overcome this difficulty, and more power could then be obtained. It should be emphasized that the cavity generally had little effect on the frequency; it served primarily as a matching device to transform the load impedance and so permit maximum power to be extracted from the specimen. The requirements for matching appear to involve the existence of a large reactive component in the load. In one case, the open- and short-circuited resonant frequencies of the cavity were measured, and from these the length at the frequency of operation was estimated to be 0.61 wavelengths.

The optimum rf power output and the corresponding input power were measured for various specimens connected in the circuit described. The peak input power was obtained from the values of pulse current and voltage measured with an oscilloscope, while the mean output power was measured by means of a conventional bolometer bridge. An rf pulse length of 200 nsec and a repetition frequency of 1 kc/sec were used. The readings of the bridge were converted to peak values by dividing by the duty cycle, 1/5000.

Values obtained in the way described above are shown in Table 3. It can be seen that those given for both power and efficiency are comparable to those for existing low-power microwave oscillators such as reflex klystrons. The peak power shown for the highest frequency in Table 3 is believed to exceed the best that has been attained with other solid state oscillators such as tunnel diodes and transistors. Were this power available continuously, rather than in brief pulses, oscillators based on the new phenomenon would have immediate practical application. However, attempts to increase the pulse length beyond about 500 nanoseconds have always led to changes in specimen resistance and to ultimate failure, apparently from thermal causes. Because of the encapsulation technique used, the conduction of heat, which occurs mainly through the epoxy resin, is at present very inefficient; calculation shows that, by the use of a heat sink, it should be possible to overcome this difficulty and to dissipate the input power of the smaller specimens continuously without undue temperature rise. Thus, if thermal limitations are the only important ones, it should ultimately be possible to utilize the new phenomenon to obtain continuous microwave power. The resulting sources would possess the advantages, common to solid state devices, of compactness, ruggedness, and low operating voltage; they would also have a very wide modulation bandwidth and a structure so simple and of such convenient dimensions that their manufacture should be relatively straightforward.

Table 3 **Peak pulse power delivered to a matched load from various specimens.**

Frequency (*Mc/sec*)	*Input* (*watts*)	*Output* (*milliwatts*)	*Efficiency* (*percent*)
950	29	550	1.9
1590	4.3	57	1.3
1670	6.0	70	1.2
1710	5.4	95	1.7
1850	3.6	25	0.7
1950	3.9	33	0.85
2730	19	155[a]	0.8

[a] Load not matched

5 Discussion

The most important problem raised by the observations is that of explaining the underlying cause of the current instability. Several different mechanisms suggest themselves; although no firm conclusions can be drawn at this stage, the implications of the experimental data can be discussed tentatively, deductions can be made a[bout] electrical circuit properties of the specimens, an[d] two untenable hypotheses about the mechanism [are] rejected.

• *5.1 Circuit properties*

A very striking feature of the experiments is the effect[ive] increasing applied voltage in producing sudden decreases in specimen current. It is remarkable that, despit[e repe]ated attempts, it was never possible to observe a dec[rease] this type that was sustained in time. This means tha[t] above the threshold the current is not simply a function of the voltage, but is also an explicit function of time. We may thus dispose of the possibility that we are dealing here with a simple negative resistance characteristic like that of a tunnel diode, in which the di[fferen]tial [resis]tance measured between the terminals is negative and essentially independent of frequency do[wn] to dc. Further support to this conclusion is given by the fact that the observed oscillations are not relaxation oscillations [but] exhibit a wide variety of wave shapes, and their pe[riod] is not correlated with the time constant L/R of the cir[cuit].

A negative conductance independent [of] [fre]quency not, of course, the only type of impeda[nce] which can be exhibited by a 2-terminal element. Elements are known for which ance is positive at zero and at most finite becoming negative over certain limited r[anges] mined by the transit time.[12] Such an elemen[t], in a circuit of suitable impedance, can generate oscil-

whose frequency necessarily lies within these limited ranges, and is thus determined primarily by the specimen and not by the circuit. In addition, the oscillations should cease when, with constant applied voltage, the external circuit impedance is reduced to a value that is small compared to the specimen resistance, or when, by a reduction of applied voltage, the negative conductance is made too weak to overcome the fixed external losses. The first of these predictions is contrary to experiment; the second implies a variation of specimen impedance with frequency which should remain noticeable near the frequency of oscillation, even when the applied voltage is reduced slightly below the threshold value. This, too, is contrary to experiment, and so we conclude that the specimen cannot be characterized by a frequency-dependent negative resistance of this type. The simplest electrical description of the specimen that would appear approximately to fit the facts is a parallel combination of a frequency-independent negative resistance (representing the tendency of the mean current to decrease, above the threshold), shunted by a constant-current ac generator whose frequency is determined mainly by the specimen length, and whose amplitude is a function of applied voltage.

ssible mechanisms

echanisms which might account for the observa- will now be considered. The discussion in this section uld not be regarded as an exhaustive catalog, for, as ill be seen, none of the effects mentioned appears to offer a completely satisfactory explanation, and it seems possible t the cause may ultimately be found in some effect as yet unknown.

T st thing to be explained is how the current can de se when the electric field *increases*; some ways in which this could happen are classified in Table 4. (Various instabilities involving the injection or multiplication of charge carriers are excluded, of course, as they would have the opposite effect.) A second important fact requiring explanation is the observed relationship between the period o tio d the electronic transit time. At present it seems pro a e that this result is, in fact, a necessary consequence of he first; however, since it is intended to discuss this poi at length elsewhere, we shall not con- s further here. Finally, we must recognize that any posed mechanism must act sufficiently rapidly to ac- nt for a current decrease of 30% in a time of 10^{-10} cond, as n in Fig. 6d.

l carrier exclusion effects

isms, namely the pinching effect on the ibution of its own magnetic field, and the f electrons by a blocking contact, can be ev at once. Although these phenomena can be tant in ambipolar transport, where electrical neutrality can be preserved, their effects are rendered negligible in the absence of mobile holes by the strong space-charge forces which oppose them. In the present case the number of intrinsic holes is negligible, and the monotonic decrease in conductivity up to the threshold field makes the injection or generation of holes seem very unlikely. An additional argument against the pinch effect is seen in the dependence of threshold conditions on specimen cross-section; it is the electric field, rather than the current, which is found to remain constant.

5.2.2 Trapping of hot electrons

Negatively charged acceptor impurity centers can exist; they present to the electrons a recombination cross-section which increases with increasing electron energy. Electrons heated by an electric field then have an increased probability of recombination, and their number decreases. This decrease may be so strong as to give rise to a negative differential conductivity.[13] Effects of this type have been observed[5] in Au-doped Ge, and probably also in semi-insulating GaAs.[14] Against this mechanism may be cited the fact that both the calculated and observed time rates of change of electron density are about 10^{-10} times those observed in the present work. Also, a rather special type of impurity is required. Although the nature of the impurities in our crystals is not known, it would be a somewhat remarkable coincidence if, into several crystals of each of two different substances, impurities of just the right type had found their way by accident. Finally, the apparent lack of any strong temperature dependence counts against a mechanism dependent on a fine balance between the energy of an electron and of a Coulomb barrier around an impurity.

5.2.3 Energy-dependent scattering of hot electrons

Electrons whose scattering rate increases as their energy increases will have an average mobility which decreases with increasing electric field. No case has been reported

Table 4 **Some mechanisms which could cause a decrease in specimen current.**

1. Decrease in current-carrying area (pinch effect)

2. Decrease in number of electrons:
a) In conduction band (trapping of hot electrons)
b) In crystal as a whole (carrier exclusion)

3. Decrease in mobility of electrons:
a) Changed relaxation time (energy-dependent scattering)
b) Changed effective mass (population of upper minima)
c) Momentum transfer to amplified wave (two stream instability, acoustical lattice modes, optical lattice modes)

hitherto in which the mobility decrease was so strong as to give rise to an actual decrease in *current*, but such a situation is not inconceivable, as may be shown by the following crude argument: Consider a fixed number of electrons, whose distribution in an electric field E may be characterized by a drift velocity v and a "temperature" T. Their mobility $\mu = v/E$ will be a function of T, say proportional to T^n. They will lose energy to the lattice (supposed to be at a temperature $\ll T$) at a rate which we may set proportional to $T \cdot A(T)$, where the energy loss coefficient A may be a function of T, say T^m. Then by equating the rate of energy loss to the rate μE^2 of input, it is readily shown[15] that the relation between v and E is

$$v \propto E^{(1+m+n)/(1+m-n)}.$$

Thus, a value of $n < -(1 + m)$ can give rise to a negative dv/dE, and probably to instabilities of the type observed. Since electronic scattering times in semiconductors are typically 10^{-11} to 10^{-12} sec, there is no difficulty in accounting for the observed speed on this hypothesis. There is, however, at present no theoretical reason to suppose that n is more negative than $-(1 + m)$. A treatment of the behaviour of hot electrons under the influence of polar scattering (which is believed[16] to be dominant in GaAs) has been given by Stratton.[17] He predicted no such effect, but found rather an unlimited increase in v at a critical field.

5.2.4 Population of upper minima in the conduction band

It has been shown[18] that a transfer of electrons, from a region of the conduction band where the effective mass is small to one where it is much greater, can lead to a negative dv/dE. The combination of a light mass at the band edge with higher-lying minima with large mass, which exists in many of the III–V compounds, can give rise to this effect when the electronic energy becomes comparable with the separation between upper and lower minima. The difficulty with this interpretation is that the energy difference is known[19] to be 0.36 eV in GaAs, and that what little evidence there is suggests[19] about 0.3 eV for InP. Thus, electronic temperatures of about 4000°K would be required. Preliminary measurements[20] show that at an electric field of 10^3 V cm^{-1}, the measured decrease in mobility and the measured noise temperature of the electrons indicate electron temperatures of about 310°K and 400°K, respectively. Since instability is observed at fields of about 1.25×10^3 V cm^{-1} in long GaAs specimens, it seems very unlikely that a significant transfer of electrons to the upper minima can have occurred at threshold. Without a more complete theory, it is not possible to say whether the speed of response of such a mechanism is adequate to explain the observations.

5.2.5 Transfer of electronic momentum to an amplified wave

There is a class of phenomena, well known in the physics of vacuum tubes and of gaseous plasmas, in which the interaction between two types of waves can give rise to instabilities, or to waves of the coupled system which grow in space or in time. The condition for the existence of such effects is that the two waves which interact should have similar but unequal phase velocities. Three rather different types of effects are known in vacuum tubes.[21] They are: (1) the two-stream instability, in which there are two space charge waves on two interpenetrating electron beams or, what is really the same thing, on a single beam with a double-humped velocity distribution; (2) traveling wave interaction between space-charge waves on an electron beam and slow electromagnetic waves on a non-dispersive structure such as a helix; and (3) backward wave interaction between an electron beam and waves on a highly dispersive periodic structure such as an interdigital line. Analogues of all three can exist in semiconductors. Under the right circumstances, strong amplification of a suitable impressed wave will occur when an electric field is applied to the semiconductor; if no wave is impressed, noise signals will build up exponentially to a large amplitude. In either case, a wave carrying a substantial quantity of momentum will appear in the theory. This momentum is derived ultimately from the electric field, which delivers it to the electrons at a fixed rate. As the wave builds up, there is an increase in the rate of transfer of momentum to it from the electrons. Less to be transferred to the lattice through collision scattering processes. The decreased momentum transfer to the lattice can come about only through a decrease in the electronic drift velocity. Thus any amplifying mechanism of this kind must give rise to a decrease in current as the wave grows from a small to a large amplitude. It should be noted that the time dependence of the current may reflect the envelope of the wave, rather than a response to individual cycles of its oscillation. Further, periodic instability in the process of amplification is analogous with the "spiking" of a laser or the oscillation of a radio-frequency oscillator, there being a corresponding periodic fluctuation in the current.

Some types of amplification

We now consider the different types of amplification that might be possible.

Two-stream instability

Although a theory of two-stream instability in semiconductors is lacking, yet we may draw some conclusions by analogy with the vacuum-tube case. There it is shown that amplification is possible if there are maxima in the velocity distribution of the electrons

electrons in a semiconductor drifting under the influence of an applied electric field, we might expect a similar effect if they can be divided into two classes with different drift velocities, the rate of scattering of electrons from one class to the other being sufficiently small. These conditions might be met for electrons in distinct valleys or sub-bands for which the relevant component of effective mass was different. Then waves with period less than the intervalley or inter-band scattering time might be amplified. For a single minimum, the rapid intravalley scattering would probably ensure stability even in the presence of a quite pathological double-humped distribution. Since both GaAs and InP have only a single minimum at the edge of the conduction band,[19] such mechanisms would appear to be unlikely.

Amplificati.n of acoustical waves

A solid state analogue of the propagation of slow electromagnetic waves along the helix of a travelling-wave tube is the transmission of acoustical modes of lattice vibration through a semiconductor; under suitable circumstances longitudinal components of both types of waves can be amplified by interactions with drifting electrons. Although ing of the electrons and the acoustical modes ... deformation potential is usually too weak in conductors to be important[22] in this context, it is ... that electrostatic coupling through a piezoelectric can give rise to large amplification effects.[23] been demonstrated experimentally.[24] Since GaAs are piezoelectric, it is conceivable that enon could be important here, especially as a ...uration ascribed to this cause has been observed[6] ... order to discuss its relevance to the present ...ts. it is necessary to adopt a somewhat wider ...n is usually taken.

...on ... bout the mutual influences of lattice waves ... ...g electrons may be obtained from a solution of th... o... ...ation for the coupled system, which gives ... ...with complex coefficients between the ... ...ve-vector q of a small-amplitude wave ... ... The usual approach[23] is equivalent to findi... ...ximation for the small quantity $\delta_1 \equiv$ ... ...ith the assumption that Im $(\omega) = 0$. ...on is appropriate for steady-state prob... wh... spatial variation of wave amplitude is calc... ...n the present case we wish to know the ... a s...tially uniform wave (e.g., a noise ...ilt u... after the sudden application of an ...c fi... ...e a... ...ropriate solution is then one for Im (... Re (... ...ith Im (q) = 0. Analysis gives a wh... migh... obtained intuitively, namely, that ... wh... e ... is the phase velocity and u the ...p vel... ...y of the w... ...e. In the present case $u/c = 1$. ...b... ...own further that the whole effect of an angular displacement between q and the electron velocity v is contained in terms of the form $\mathbf{q}\cdot\mathbf{v}$. Thus, we may obtain the relation

$$\omega_2 = \frac{K^2_{\mathbf{q},\mathbf{p}}\omega_c\omega_1}{8\pi}\cdot\frac{(\mathbf{q}\cdot\mathbf{v}-\omega_1)}{(\mathbf{q}\cdot\mathbf{v}-\omega_1)^2+(\omega_c+Dq^2)^2}$$

for a wave propagating with real wave-vector q, angular frequency of oscillation ω_1, and rate of growth proportional to $\exp(\omega_2 t)$. Here D is the diffusion constant of electrons and $\omega_c = 4\pi\sigma/\epsilon$ is the dielectric relaxation frequency of the semiconductor. The electromechanical coupling constant for the wave whose polarization vector is p is denoted by $K^2_{\mathbf{q},\mathbf{p}}$. By the use of the equation $q = \omega_1/c$, this may be put in the form

$$\omega_2 = \frac{K^2_{\mathbf{q},\mathbf{p}}\omega_c}{8\pi}\cdot\frac{\left(\frac{v}{c}\cos\theta-1\right)}{\left(\frac{v}{c}\cos\theta-1\right)^2+\left(\frac{\omega_c}{\omega_1}+D\omega_1/c^2\right)^2}.$$

Since noise components with a wide range of frequencies will be present at the instant when the electric field is applied, the value of ω_1 is to be chosen, not according to some specified input, but so as to maximize ω_2. This value, $\omega_1' = (c^2\,\omega_c/D)^{\frac{1}{3}}$, is the frequency of the fastest growing and hence eventually dominant wave. The corresponding growth rate, given by

$$\omega_2' = \frac{K^2_{\mathbf{q},\mathbf{p}}\,\omega_c}{8\pi}\cdot\frac{\left(\frac{v}{c}\cos\theta-1\right)}{\left(\frac{v}{c}\cos\theta-1\right)^2+4D\omega_c/c^2},$$

should then set the time-scale on which noticeable effects of the amplification of acoustical waves should appear.

The value of ω_2' given by the last equation is still undetermined to the extent that it depends on the direction of q through the angle θ, and through the variation with q of the coupling coefficient $K^2_{\mathbf{q},\mathbf{p}}$. Again we must look for the maximum. Although the latter variation is quite large ($K^2_{\mathbf{q},\mathbf{p}} = 0$ for some cases), we shall see that it is the largest possible value of ω_2 that is of interest, so that it is sufficient to set $K^2_{\mathbf{q},\mathbf{p}}$ equal to its greatest value K^2. Then the effect of varying θ depends on whether or not v exceeds a certain value v_1. For $v > v_1$, $\omega_2'(\theta)$ has a maximum at a finite value of θ; this value tends to $\pi/2$ as $v \to \infty$. For $v < v_1$, the maximum always occurs at $\theta = 0$. Correspondingly, the maximum value of ω_2' is dependent on v for $v < v_1$, but not for $v > v_1$. The value of v_1 is given by

$$v_1 = c + 2(D\omega_c)^{1/2}.$$

For material typical of the present experiments, we have $D \sim 130\ \mathrm{cm^2\,sec^{-1}}$, $\omega_c \sim 3\times10^{12}\ \mathrm{sec^{-1}}$, so that $v_1 \sim c + 4\times10^7\ \mathrm{cm\ sec^{-1}}$. Thus, the experimental values of v lie

in the range $v < v_1$, where the fastest growing wave propagates in a direction parallel to the electron current. (This conclusion neglects, of course, the angular dependence of $K^2_{q,p}$.) In fact, we can make the approximation $(v - c)^2 \ll v_1^2$, and in that case the maximum, ω_2'', of ω_2' as a function of θ, is given approximately by

$$\omega_2'' = \frac{K^2 c(v - c)}{32\pi D}$$

and is independent of ω_c. The value of ω_1 associated with this fastest-growing wave is in the present case about 5×10^{10} sec^{-1}. Waves of other frequencies will grow more slowly.

The value of the coupling constant $K^2_{110,1\bar{1}0}$ has been given [25] as equal to 2.4×10^{-3} for GaAs. Then, for an electron drift velocity of $v = 10^7$ cm sec^{-1} and sound velocity[26] of $c = 3.4 \times 10^5$ cm sec^{-1}, we find the value $\omega_2 = 6 \times 10^5$ sec^{-1}.

This means that under the conditions of our experiment even the fastest-growing sound wave takes 1.7 microseconds to increase in amplitude by a factor of $e = 2.718 \cdots$ Since the time for the conductivity to change by a comparable amount is found to be in the range 10^{-10} to 10^{-9} sec, it is clear that the observed instabilities of current do not represent non-linear effects of the growing amplitude of sound waves. Furthermore, since the oscillations themselves grow to full amplitude in a time of the order of 10^{-9} sec, it is equally impossible to make a correspondence between individual cycles, of the current oscillations on the one hand, and of an amplified sound wave on the other. A further argument against this last possibility is that the measured relationship between frequency and specimen length would imply a phase velocity of sound equal to 10^7 cm sec^{-1}. Finally, the absence of persistence effects shows that the decay time of any waves which may be involved is less than 10^{-9} sec. Thus, we conclude that the amplification of sound waves is unlikely to be the cause of the observed current instabilities.

Amplification of lattice optical waves

Longitudinal optical modes of vibration constitute a second type of lattice wave with which drifting electrons may interact.[26,27] Here there is a strong analogy with the amplification of an electromagnetic wave on the dispersive structure of a backward-wave tube. In both cases the group velocity (and hence the direction of amplification) is directed oppositely to the phase velocity of the wave. Since the frequency of the optical modes in GaAs is of the order[28] of 10^{13} sec^{-1}, it is clear that there cannot be a cycle-by-cycle correspondence between the observed oscillations and optical vibrations. If the latter are involved, it must therefore be fluctuations in their amplitude that are reflected in the oscillating specimen current. Once again we ask whether the time rate of growth of these waves can be great enough to account for the observed frequencies of oscillation. Even if it can be, some other mechanism is, of course, still needed to explain why the amplitude, once built up, should die away again, allowing the current to build up again, and the process to be repeated cyclically.

A theory of the amplification of optical modes has been given,[26] which is based on the use of the classical equations of lattice dynamics (modified to give a realisti dispersion law) and on macroscopic equations of carrier transport. While this way of treating carrier-lattice interactions is open to doubts, discussed below, the results are perhaps of the correct order of magnitude. The amplitude of an optical mode is found to change proportionately to exp $\omega_2 t$, with ω_2 given approximately by

$$\omega_2 = \frac{\omega_1 \omega_c}{2}\left(1 - \frac{\epsilon_\infty}{\epsilon_0}\right)\frac{(\mathbf{q}\cdot\mathbf{v} - \omega_1)}{(\mathbf{q}\cdot\mathbf{v} - \omega_1)^2 + (Dq^2 + \omega_c)^2}$$

Here $\mathbf{q}$ is the wave-vector and ω_1 is the (essent angular frequency of the optical mode, ϵ_∞ and ϵ_0 high- and low-frequency dielectric constants of the rial, and ω_c, $\mathbf{v}$, and D have the same mean. Just as in the acoustical case, one wave grow any other; its wave-vector is given by

$$q = 4\omega_1/3v,$$

and its rate of growth by

$$\omega_2 = 3^3 \cdot 2^{-9} \omega_c v^4 [1 - (\epsilon_\infty/\epsilon_0)]/D\omega_1^2$$

provided the conditions

$$D\omega_1^2/v^2 \gg \omega_1 \gg \omega_c, \qquad d\omega/dq \ll v$$

are fulfilled. These requirements are met i case.

Because changes in the electron curr result only of nonlinear effects of the e citation, we should expect them to as the square of the optical mod the relevant growth rate is $2\omega_2$. In graph of $2\omega_2$ against v, calculated from using the values[28,29] $\epsilon_0 = 12.5$, $\epsilon_\infty = 10$ and D and ω_c as given in the previous s graph is shown approximately the regio experimental points representing frequency of plotted against measured drift velocity. Now $(2\omega_2)^{-1}$ is the period needed for the disturbanc tron current by the optical modes to gr $e = 2.718$. Obviously, the time for a com cycle involving the growth and dec y modes must be greater than this. Thu , fo nism to be credible, the shaded r gio n should the theoretical curve. As will be seen, it lies above, the calculated rate of amplificatio des

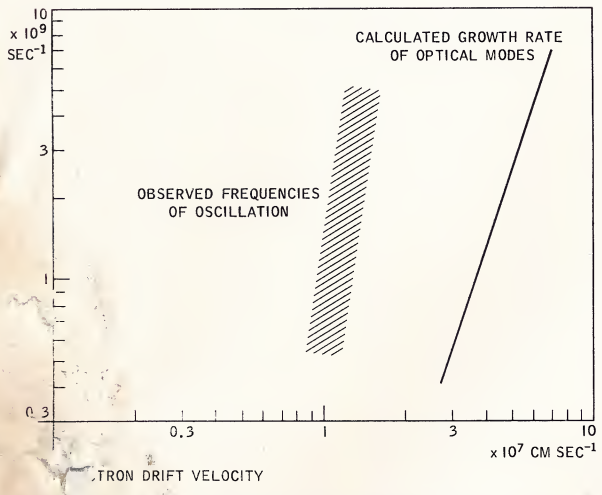

Figure **Comparison between calculated rate of growth of optical modes and the observed frequencies of oscillation for GaAs.**

itly great to account for the observations. It would, ably be unwise to reject the mechanism com- is point, in view of the approximate nature of . Its derivative neglects, among other things, the relaxation time of the electrons is not ble compared with the (Doppler-shifted) opti- iod, and that quantum effects may be impor- quencies in question. It may be noted further h Fig. 13 shows a large discrepancy between and observed rates of growth at a given drift threefold increase in velocity would bring view of the fact that the measured electronic ity of $\sim 10^7$ cm sec^{-1} is comparable to the mal velocity of 2.5×10^7 cm sec^{-1}, the tion existing just below the threshold field nMaxwellian. In that case, it is quite fective drift velocity which should be cation formula is greater than the

Acknowledgments

The author is indebted to many of his colleagues for advice and assistance. In particular, it is a pleasure to thank J. L. Staples for his untiring help with the experiments, C. A. Bryant for communicating his data before publication, S. E. Blum and J. M. Woodall for the supply of crystals, and P. J. Price for helpful discussions.

References and footnotes

1. E. J. Ryder, *Phys. Rev.* **90**, 766 (1953).
2. E. Erlbach and J. B. Gunn, *Phys. Rev. Letters* **8**, 280 (1962).
3. K. G. McKay and K. B. McAfee, *Phys. Rev.* **91**, 1079 (1953).
4. E. J. Ryder, I. M. Ross and D. A. Kleinman, *Phys. Rev.* **95**, 1342 (1954).
5. B. K. Ridley and R. G. Pratt, *Phys. Letters* **4**, 300 (1963).
6. R. W. Smith, *Phys. Rev. Letters* **9**, 87 (1962).
7. L. Esaki, *Phys. Rev. Letters* **8**, 4 (1962).
8. C. Zener, *Proc. Roy. Soc.* **A145**, 523 (1934).
9. A brief preliminary account has been published elsewhere: J. B. Gunn, *Solid State Communications* **1**, 88 (1963).

10a. 3 H_2SO_4 : 1 H_2O_2 : 1 H_2O.

10b. 17 drops Br_2 : 10 cm^3 CH_3OH.

11. J. B. Gunn, *Proc. Phys. Soc.* (*London*) B, **69**, 781 (1956).
12. W. Shockley, *Bell Syst. Tech. J.* **33**, 799 (1954).
13. B. K. Ridley and T. B. Watkins, *Proc. Phys. Soc.* (*London*) **78**, 710 (1961).
14. A. Barraud, *Compt. Rend.* **256**, 3632 (1963).
15. K. J. Schmidt-Tiedemann, private communication.
16. H. Ehrenreich, *Phys. Rev.* **120**, 1951 (1960).
17. R. Stratton, *Proc. Roy. Soc.* **A246**, 406 (1958).
18. B. K. Ridley and T. B. Watkins, *Proc. Phys. Soc.* (*London*) **78**, 293 (1961).
19. H. Ehrenreich, *J. Appl. Phys.* **32**, 2155 (1961).
20. C. A. Bryant, private communication.
21. A. H. W. Beck, *Space Charge Waves*, Pergamon Press, New York, 1958.
22. G. Weinreich, *Phys. Rev.* **104**, 321 (1956).
23. D. L. White, *J. Appl. Phys.* **33**, 2547 (1962).
24. J. H. McFee, *J. Appl. Phys.* **34**, 1548 (1963).
25. A. R. Hutson and D. L. White, *J. Appl. Phys.* **33**, 40 (1962).
26. J. B. Gunn, *Phys. Letters* **4**, 194 (1963).
27. V. L. Gurevich, *Soviet Phys.—Solid State* **4**, 1015 (1962).
28. F. A. Johnson and W. Cochran, *Proc. Int. Conf. Semiconductor Physics*, Exeter, 1962, p. 498.
29. K. G. Hambleton, C. Hilsum and B. R. Holeman, *Proc. Phys. Soc.* (*London*) **77**, 1147 (1961).

Received December 24, 1963.